The power of pure shift HαCα correlations: a way to characterize biomolecules under physiological conditions

Andrea Bodor, Jens D. Haller, Chafiaa Bouguechtouli, Francois-Xavier Theillet, László Nyitray, Burkhard Luy

The power of pure shift HαCα correlations: a new way to characterize biomolecules under physiological conditions

Andrea Bodor*[a], Jens D. Haller[b], Chafiaa Bouguechtouli[c], Francois-Xavier Theillet[c], László Nyitray[d], Burkhard Luy*[b]

[a] Eötvös Loránd University, Institute of Chemistry, Pázmány Péter sétány 1/a, Budapest 1117, Hungary
E-mail: abodor@caesar.elte.hu

[b] Institut für Organische Chemie and Institut für Biologische Grenzflächen 4 – Magnetische Resonanz, Karlsruher Institut für Technologie (KIT), Fritz-Haber-Weg 6, 76133 Karlsruhe, Germany

E-mail: Burkhard.Luy@kit.edu

[c] Institute of Integrative Biology of the Cell, UMR9198, CNRS/CEA/ Univ. Paris Saclay, 911991 Gif-Sur-Yvette, France

[d] Eötvös Loránd University, Department of Biochemistry, Pázmány Péter sétány 1/c, Budapest 1117, Hungary

KEYWORDS. *NMR spectroscopy • selective HSQC • Hα detection• homonuclear decoupling • IDP*

ABSTRACT: Intrinsically disordered proteins (IDPs) constitute an important class of biomolecules with high flexibility. Atomic resolution studies for these molecules are essentially limited to NMR spectroscopy, which should be performed under physiological pH and temperature to populate relevant conformational ensembles. In this context, however, fundamental problems arise with established triple resonance NMR experiments: high solvent accessibility of IDPs promotes water-exchange, which disfavors classical amide ^{1}H-detection, while ^{13}C-detection suffers from significantly reduced sensitivity. A favorable alternative, the conventional detection of non-exchangeable ^{1}Hα, so far resulted in broad signals with insufficient resolution and sensitivity. To overcome this we introduce here a selective Hα,Cα-correlating pure shift detection scheme, the SHACA-HSQC, using extensive hetero- and homo-nuclear decoupling applicable to aqueous samples (≥ 90% H_2O) and tested on small molecules and proteins. SHACA-HSQC spectra acquired on IDPs provide uncompromised resolution and sensitivity (up to 5-fold increased S/N compared to the standard ^{1}H,^{13}C-HSQC), as shown for resonance distinction and unambiguous assignment on the disordered transactivation domain of the tumorsuppressor p53, α-synuclein, and folded ubiquitin. The detection scheme can be implemented in any ^{1}Hα-detected triple resonance experiment, but may also form the basis for the detection of isotope-labeled markers in biological studies or compound libraries.

INTRODUCTION

To elucidate biological function, state-of-the-art protein characterization is the most relevant if performed at physiological conditions. Solution NMR spectroscopy offers residue and atomic level information and it is the only technique to directly obtain this detailed characterization for the class of highly flexible, intrinsically disordered proteins (IDPs).[1-3] IDPs generally lack a hydrophobic core and do not possess defined secondary or tertiary structure, but rather have the propensity to form transient active conformations.[4] They are involved in many cellular processes (regulation, transcription, apoptosis) and intrinsic disorder is frequently detected in case of proteins associated with various human diseases.[5-6] For a sound structural characterization it is indispensable to measure close to physiological conditions and with the highest possible sensitivity to identify full structural ensembles including potentially active, low-populated conformers. The established protein NMR methods based on amide proton (^{1}HN) detection were developed for folded biomolecules. The large solvent-accessibility of IDPs under physiological pH and temperature leads to undetectable signals due to the exchange of ^{1}HN with water protons.[7-8] In addition, important proline residues – abundantly present in IDPs[4, 9-10] – cannot be detected due to the lack of an HN proton. Thus, there is a need for different approaches, and current methods specifically designed for IDPs are based on ^{13}C [11-15] or Hα detection,[16-19] with well-known disadvantages. ^{13}C-detected experiments come with low sensitivity, thus limiting the applications

to the detection of major conformers. Common Hα-detected experiments suffer from broad signal widths in both ^{1}H and ^{13}C dimensions, leading to low resolution and low sensitivity. Surprisingly, it turns out that the signal widths for highly flexible ^{13}C,^{15}N-labeled IDPs is almost exclusively caused by very large multiplets, while underlying natural linewidths are generally narrow. Hence, our aim was to explore this property and to provide a widely applicable, extensively decoupled Hα-detected "pure shift" acquisition scheme with both vastly increased sensitivity and resolution. With the resulting approach we hope to enable a deeper characterization of IDPs and folded proteins under physiological conditions in aqueous solution, enabling at the same time the detection of minor conformers present at low concentrations. Nevertheless, the scheme will also be of interest for diverse studies based on isotopically enriched small molecules, as we demonstrate using the free amino acids.

EXPERIMENTAL SECTION

NMR spectra were recorded at 303K on a 600MHz Bruker Avance III spectrometer equipped with a 5mm ^{1}H/^{13}C/^{15}N TCI cryogenically cooled probehead, and a Bruker Avance III spectrometer operating at 700.05MHz, equipped with a 5mm Prodigy TCI H&F-C/N-D, z-gradient probehead. A commercially available U-^{13}C/^{15}N labeled amino acid mixture sample containing variable amounts from each amino acid (Sigma Aldrich) was measured in D_2O. The composition of the U-^{13}C/^{15}N labeled aqueous protein samples was: 1mM p53TAD$^{1-60}$,150mM NaCl, 10% D_2O, pH=6.5;[20] 1.5mM His-Ubi, 25mM KH_2PO_4, 10% D_2O, pH=4.6; 200μM AS in PBS, pH=7.2, 5% D_2O; 50μM AS in PBS, pH=7.2, 5% D_2O. Details to individual experiments are given in the SI.

RESULTS AND DISCUSSION

For the advantage of pure shift spectra compared to coupled spectra, the multitude of homo- and heteronuclear couplings that arise in the isotopically labeled amino-acids and proteins has to be considered (Figure 1a). The selective Hα,Cα-HSQC (simply referred to as SHACA-HSQC in the following) pulse sequence introduced in Figure 1b,c constructively uses ^{1}H and ^{13}C polarization and, following the original band-selective decoupling by the Ernst group,[21] provides a specifically designed decoupling element during Cα-evolution (Figure 1b, red box, and Figure 1d); all couplings except the very small $^{3}J_{C\alpha C\alpha}$ and the $^{1}J_{C\alpha C\beta}$ of serines – for which band-selective pulses cannot separate their Cα and Cβ chemical shifts – are removed. The directly detected dimension involves pure shift acquisition, *i.e.* full reduction of multiplets by simultaneous homo- and heteronuclear decoupling. From the multitude of reported homonuclear decoupling elements,[22-45] only real-time decoupling using band-selective HOBS[35], BASHD[38], or the recently published BASEREX[45] qualify for sensitive detection of Hα protons. HOBS and BASHD both rely on a train of Hα- selective refocusing pulses that strongly affect the water resonance. BASEREX, instead, is band-selective on the X-nucleus and artefacts due to the radiation damping of water can be avoided by simultaneously applying weak gradients and hard pulses (Figure 1b,c, blue box, and Figure 1e). The modified BASEREX acquisition scheme also allows a dramatic reduction of the required heteronuclear decoupling power, thus acquisition times exceeding half a second are enabled to obtain highest resolution. The sequence provides singlets to all Hα protons except the ones belonging to glycines, for which the geminal $^{2}J_{H\alpha H\alpha}$ leads to doublets.

The performance of the pulse sequence was tested on a uniformly ^{13}C/^{15}N-labeled amino acid mixture, the disordered transactivation domain of the tumor suppressor p53 protein (p53TAD$^{1-60}$), disordered α-synuclein (AS, 140aa) and folded His-tagged ubiquitin (His-Ubi, 82aa). The amino acid mixture was used for initial implementation and evaluation of the sequence, and fully decoupled, very sharp lines of less than 1Hz (^{13}Cα) and 2.5Hz (^{1}Hα) could be obtained (Figure S1).

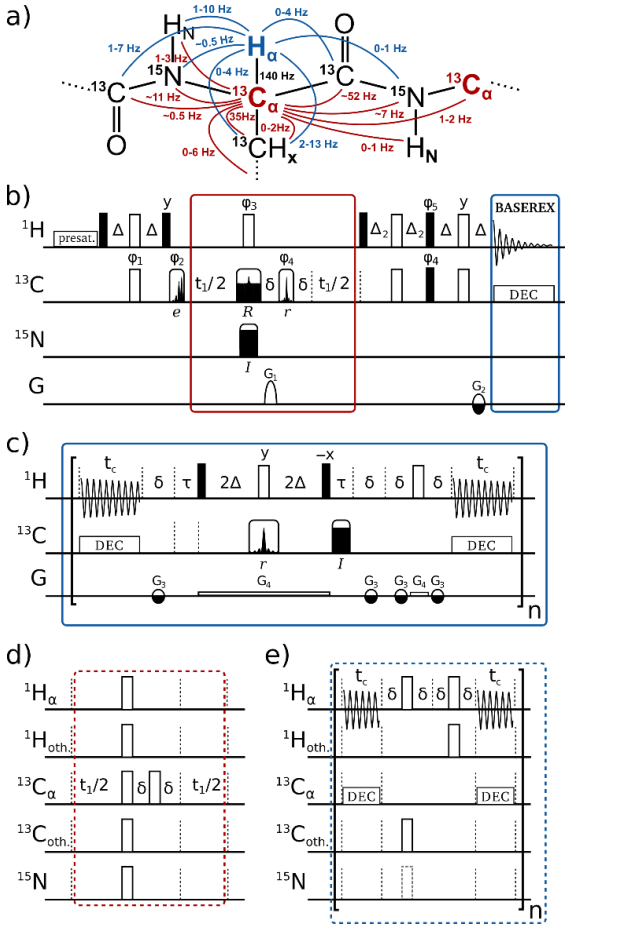

Figure 1. Homo- and heteronuclear decoupled Hα,Cα-selective SHACA-HSQC. (a) The typical coupling network of Hα and Cα environments in proteins; (b) the pulse sequence - red and blue boxes mark the decoupling elements in the indirectly and directly detected dimensions; (c) the gradient-enhanced BASEREX acquisition scheme with homo- and heteronuclear real-time decoupling; (d) and (e) schematic pulse sequence for decoupling during Cα-evolution and BASEREX-acquisition. Filled narrow bars correspond to 90° and wide open bars to 180° hard pulses, respectively. Broadband and Cα-selective shaped pulses are indicated by

upper and lowercase letters, *R:* BURBOP refocusing pulse covering the full ^{13}C-bandwidth,[46-47] *I*: a BIP[48] or BIBOP[49-51] inversion pulse covering the full ^{13}C and the ^{15}N amide bandwidth, *e:* EBURP excitation pulse[52], *r*: REBURP refocusing pulse[45, 52]. Delay Δ is set to 1/(4 $^1J_{CH}$), while Δ_2 is set to 1/(4 $^1J_{CH}$) for residues with CH groups in the α-position and 1/(8 $^1J_{CH}$) is the optimized value for –CH_2– groups. Pulse phases are x unless indicated otherwise. ϕ_1=x, ϕ_2=x,-x, ϕ_3=2(x),2(-x), ϕ_4=4(x),4(-x), ϕ_5=-y, ϕ_{rec}=x,-x,x,-x,x,-x,x,-x. The gradient ratio G_1/G_2 is set to 80:±20.1 for ^{13}C coherence order selection. Gradients G_3 and G_4 are typically set to 9% and 0.1% of the maximum strength and are applied with alternating sign for each chunking period. Echo/antiecho detection is achieved by cycling ϕ_1, ϕ_2, ϕ_{rec} and the gradient G_2. Depending on the overall acquisition time, *n*=8-20 periods with chunk times t_c of 9-13.5ms have been used for acquisition.

Next, the dramatic gain in resolution caused by the different decoupling schemes can be highlighted on the various spectra measured on the IDP p53TAD[1-60]. A comparison for the proline region encompassing 9 out of the 10 proline Cα resonances is shown in Figure 2. The commonly used state-of-the-art experiment for Hα-detection is a constant time HSQC.[53] Here the unavoidable signal loss due to the multitude of long-range ^{13}C,^{13}C-couplings limits the duration of constant time periods.

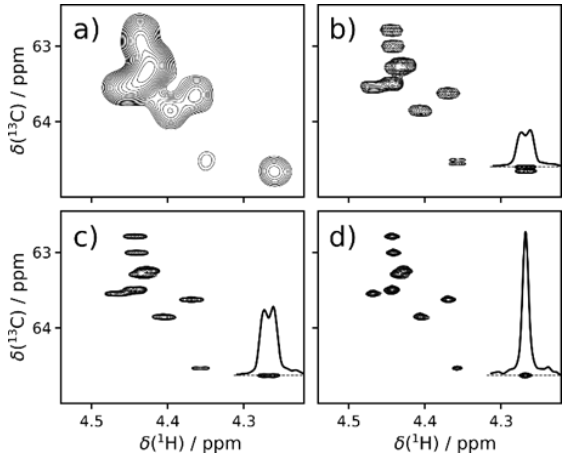

Figure 2. The proline region of p53TAD[1-60] recorded using a (a) conventional CT-HSQC, (b) selective HSQC with ^{1}H and ^{13}C decoupling in the indirect dimension, (c) with ^{1}H, ^{13}C, and ^{15}N decoupling in the indirect dimension and (d) full hetero- and homonuclear decoupling in both dimensions. The increase in signal intensity is shown on the traces for a selected proline residue.

Accordingly, commonly used periods allow only rough resolution in the indirect dimension and proline signals cannot be resolved (Figure 2a). The situation is changed by introducing Cα-selective decoupling, which allows acquisition of much better resolved spectra, and is additionally improved by simultaneous decoupling of $^1J_{C\alpha N}$ and $^2J_{C\alpha N}$ couplings using a ^{15}N broadband inversion pulse during t_1 (Figure 2b, c). Finally, application of the modified BASEREX homo- and heteronuclear decoupling scheme during acquisition (Figure 2d) results in a significant improvement in spectral quality (see also Figure S2).

A second example demonstrating the performance of the SHACA-HSQC is the biologically relevant AS, an IDP containing seven imperfect KTKE(Q)GV repeat sequences with particularly low NMR signal dispersion. As seen in Figure 3 (and Figure S3) most residues are resolved, even in critical regions - shown as inlets for 17 out of 19 alanines and 18 out of 19 valines.

A closer examination of the SHACA-HSQC spectra for both IDPs shows that ^{1}H and ^{13}C signal widths (SW) are relatively uniform, being 7-9 Hz and 6-8 Hz, respectively. Knowing that the typical signal dispersion (SD) of an IDP is within 1 ppm (^{1}Hα) and 16 ppm (^{13}Cα, excluding glycines), the corresponding average resolution of SHACA-HSQC is comparable to that of the ^{13}C-detected CON and it is higher than the average resolution of the ^{1}H,^{15}N-HSQC experiments (see Table 1).

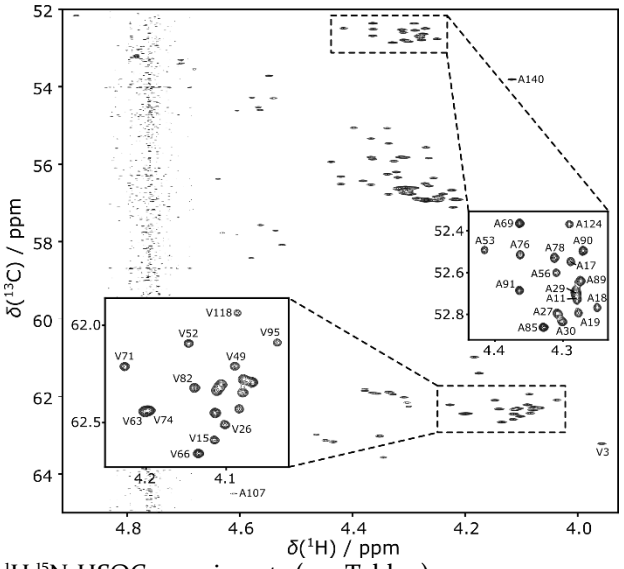

Figure 3. SHACA-HSQC measured on 200μM AS in 90% H_2O/10% D_2O.The spectrum with 2k x 512 complex points and 4 scans/increment was recorded in 1h25min. Insets show zooms of the alanine and valine regions.

Table 1. Resolution of typical 2D measurements: signal dispersion (SD) at 700MHz and measured signal width (SW) ranges.

Experiment	Direct dimension SD(Hz)	SW(Hz)	Indirect dimension SD(Hz)	SW(Hz)
^{1}H,^{15}N-HSQC	700	4.5-13	1680	7-15
CON	1050	7-10	2450	4.5-13
SHACA-HSQC	700	7-9	2800	6-8

Furthermore, there is the general belief that for a good quality Hα-detected measurement the protein should be dissolved in pure D_2O. In this work all samples were measured in aqueous solutions with a minimum of 90%

H_2O content. With well-shimmed samples the residual water artefacts are of distinctly lower intensity than the corresponding protein signals and even signals very close to the water frequency can be unambiguously identified (Figure 4a).

As has been reported previously,[54] non-proline Cα resonances experience a deuterium isotope shift for the fraction of deuterated amide groups. In the highly resolved SHACA-HSQC spectra these minor signals are detectable 100 ppb upfield from the major signal (Figure 4b) for slow-exchanging amides.

Besides the enhanced resolution, SHACA-HSQC spectra show an improved and generally high sensitivity. The sensitivity gain due to decoupling is shown on the slices of P60 in Figure 2b-d. An even more impressive example is shown in Figure 4b for signals of the deuterium isotope shifted fractions at concentrations ≤2.5μM recorded in 42 minutes. Note, as proton/deuteron (-NH/D_2O) exchange is not the same for all residues, the isotope shifted minor signals will not be detected for all of them, moreover the intensities of these signals can vary as well – as seen in Figure 4b.

In general, decoupling during t_1 is applied without noticeable signal loss and will always lead to an increased signal-to-noise ratio.

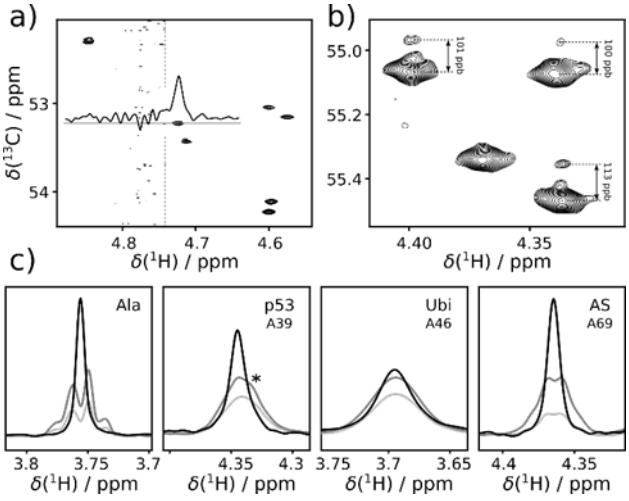

Figure 4. Performance of the water suppression and signal intensities. (a) Spectral region around the water resonance acquired on p53TAD1^{-60} in 90% H_2O/10% D_2O; a trace through the signal closest to the water resonance is given and a dashed line indicates the frequency used for presaturation. (b) Spectral region from a SHACA-HSQC acquired in 42 minutes on 50μM AS in 95% H_2O/5% D_2O showing isotope-shifted cross peaks. (c) Comparison of Ala signals obtained from SHACA-HSQC experiments with ^{1}H,^{13}C-decoupling during t_1 (light gray), ^{1}H,^{13}C,^{15}N-decoupling during t_1 (gray), and full decoupling in both dimensions (black) acquired on the free amino acid, p53TAD$^{1-60}$ (peak overlap with a neighboring signal for p53 is indicated by an asterisk), His-Ubi and AS.

BASEREX homodecoupling, on the other hand, typically involves 8-20 additional transfer steps of approximately 9ms duration during which signal decays due to relaxation. This can be an impediment for large globular proteins with short T_2 relaxation times and result in severe signal losses, while small folded proteins and IDPs of any size will benefit. To establish the limits for applicability we closely examined the intensity gain resulting from homo- and heteronuclear decoupling measured on a defined spin system. Figure 4c-f shows respective 1D slices for alanine as the free amino acid as well as in selected alanines from p53TAD$^{1-60}$, His-Ubi and AS. In all cases an increase in S/N is observed for decoupling in both dimensions. In theory, ^{15}N-decoupling in the indirect dimension should lead to doubled signal intensities, while homonuclear decoupling in the direct dimension causes the collapse of the 1:3:3:1 quartet (having a neighboring –CH_3 group) to a single line with an intensity increase of 8/3, altogether leading to a maximum gain of approximately 5.3. In our case both the free amino acid and AS reach the theoretical value. Folded His-Ubi, however, shows an overall gain of 2.1 and the dynamically broadened p53-TAD$^{1-60}$ lies in between with an overall gain of approximately 2.8. We conclude that decoupling results in up to 5-fold increased S/N compared to the standard ^{1}H,^{13}C-HSQC. The theoretical gain in sensitivity is achieved as long as the non-decoupled multiplets can be identified (as for the free amino acid and AS), while signals without an identifiable multiplet structure (as in His-Ubi and p53TAD$^{1-60}$) will lead to smaller improvements. Discussion for multiplicities originating from -CH_2- or -CH- neighbors illustrated by selected Pro and Ile are shown in Figure S4. Overall, we expect gains for folded proteins consisting of up to about 100 residues, while for larger globular molecules one should record the SHACA-HSQC without BASEREX homodecoupling.

Due to its spin system, the pulse sequence in the presented form hinders the detection of glycines, which can be overcome by adjusting the Δ_2 back-transfer delay to $1/(8\,{}^1J_{CH})$ and by shifting the irradiation frequency of the selective pulse, though the splitting due to the geminal $^2J_{H\alpha H\alpha}$ coupling will still remain (see SI for details).

CONCLUSIONS AND PERSPECTIVE

The presented selective, extensively decoupled HαCα correlation experiment is suitable for isotopically labeled small molecules and proteins in aqueous solution. High resolution spectra can be achieved in approximately 40 minutes or less if non-uniform sampling is applied (see Figure S2). The resulting peak distancing - especially for the study of crowded IDP spectra - makes both automatic and manual peak picking possible and more accurate.

The obtained resolution is comparable to ^{13}C-detected CON experiments (see Table1), however with enhanced sensitivity. On a 700MHz spectrometer equipped with a Prodigy cryogenically cooled TCI probehead the relevant ratio S/(N$\sqrt{t}$) of the SHACA-HSQC compared to the CON

experiment revealed a minimum sensitivity increase of 7. This implies that the ^{13}C-detected experiment has to be run $7^2 \approx 50$ times longer to obtain the same S/N ratio. This represents a major gain in experimental time and feasibility.

Compared to $^{1}H,^{15}N$-HSQC experiments as the standard work horse of current protein NMR measurements, the SHACA-HSQC provides higher resolution, with the addition that the important proline residues are no longer missing and spectral quality is much less affected by pH and temperature, thus work at physiological conditions is possible.

Moreover, all protein spectra were acquired in aqueous solution with D_2O contents as low as 5% in 5mm standard NMR tubes. For 200μM IDP samples signals very close to the water could straightforwardly be identified, so that no special sample treatment is needed. Further reduction of residual H_2O artefacts is expected with the use of lower volume or shaped NMR tubes, but has not been tested here.

All these properties make the new SHACA-HSQC attractive to be used as an essential reference, which is ready for incorporation into 3D-type sequences to provide a complete set of triple-resonance experiments for uncompromised studies of IDPs. It will allow to address special structural questions, like for example the residue-specific identification of post-translational modifications,[55] with utmost spectral resolution and sensitivity. Furthermore, the general approach of the presented band-selective pure-shift spectra can be of use in all types of chemical, biological or pharmaceutical applications involving molecules with high abundance of NMR-active isotopes, including reaction monitoring, the characterization of compound libraries, or the determination of metabolic pathways.[56-58]

ASSOCIATED CONTENT

Supporting information for the amino-acid mixture, $p53TAD^{1-60}$, AS; comparison of proline and isoleucine signals from the different proteins; experimental details; the SHACA pulse sequence.

AUTHOR INFORMATION

Corresponding Authors

Andrea Bodor – Eötvös Loránd University, Institute of Chemistry, Pázmány Péter sétány 1/a, Budapest 1117, Hungary
E-mail: abodor@caesar.elte.hu

Burkhard Luy - Institut für Organische Chemie and Institut für Biologische Grenzflächen 4 – Magnetische Resonanz, Karlsruher Institut für Technologie (KIT), Fritz-Haber-Weg 6, 76133 Karlsruhe, Germany
E-mail: Burkhard.Luy@kit.edu

ACKNOWLEDGEMENT

This work was completed in the ELTE Institutional Excellence Program supported by the National Research, Development and Innovation Office (NKFIH-1157-8/2019-DT). Financial support by the NKFI Grants K124900, K119359 the Deutsche Forschungsgemeinschaft (DFG LU 835/11-1 and LU 835/13-1) and the HGF program BIFTM (47.02.04) is also acknowledged.

ABBREVIATIONS

IDP, intrinsically disordered protein; SHACA-HSQC, selective Hα,Cα-HSQC.

REFERENCES

1. Dyson, H. J.; Wright, P. E., Unfolded Proteins and Protein Folding Studied by NMR. Chem. Rev. 2004, 104, 3607-3622.
2. Kosol, S.; Contreras-Martos, S.; Cedeño, C.; Tompa, P., Structural Characterization of Intrinsically Disordered Proteins by NMR Spectroscopy. Molecules 2013, 18, 10802-10828.
3. Felli, I. C.; Pierattelli, R., Intrinsically Disordered Proteins Studied by NMR Spectroscopy. Springer International Publishing: Cham, 2015; Vol. 870, p 1-421.
4. Uversky, V. N., Intrinsically Disordered Proteins and Their "Mysterious" (Meta)Physics. Front. Phys. 2019, 7, 8-23.
5. Uversky, V. N.; Davé, V.; Iakoucheva, L. M.; Malaney, P.; Metallo, S. J.; Pathak, R. R.; Joerger, A. C., Pathological Unfoldomics of Uncontrolled Chaos: Intrinsically Disordered Proteins and Human Diseases. Chem. Rev. 2014, 114, 6844-6879.
6. Tompa, P.; Fersht, A., Structure and Function of Intrinsically Disordered Proteins. Chapman and Hall/CRC: 2009; p 1-333.
7. Pérez, Y.; Gairí, M.; Pons, M.; Bernadó, P., Structural Characterization of the Natively Unfolded N-Terminal Domain of Human c-Src Kinase: Insights into the Role of Phosphorylation of the Unique Domain. J. Mol. Biol. 2009, 391, 136-148.
8. Murrali, M. G.; Schiavina, M.; Sainati, V.; Bermel, W.; Pierattelli, R.; Felli, I. C., 13C APSY-NMR for sequential assignment of intrinsically disordered proteins. J. Biomol. NMR 2018, 70, 167-175.
9. Theillet, F.-X.; Kalmar, L.; Tompa, P.; Han, K.-H.; Selenko, P.; Dunker, A. K.; Daughdrill, G. W.; Uversky, V. N., The alphabet of intrinsic disorder. Intrinsically Disord. Proteins 2013, 1, e24360.
10. Mateos, B.; Conrad-Billroth, C.; Schiavina, M.; Beier, A.; Kontaxis, G.; Konrat, R.; Felli, I. C.; Pierattelli, R., The Ambivalent Role of Proline Residues in an Intrinsically Disordered Protein: From Disorder Promoters to Compaction Facilitators. J. Mol. Biol. 2019.
11. Bermel, W.; Felli, I. C.; Kümmerle, R.; Pierattelli, R., 13C Direct-detection biomolecular NMR. Concepts Magn. Reson. A 2008, 32A, 183-200.
12. Bermel, W.; Bertini, I.; Chill, J.; Felli, I. C.; Haba, N.; Kumar M. V., V.; Pierattelli, R., Exclusively Heteronuclear 13C-Detected Amino-Acid-Selective NMR Experiments for the Study of Intrinsically Disordered Proteins (IDPs). ChemBioChem 2012, 13, 2425-2432.
13. Felli, I. C.; Pierattelli, R., Novel methods based on 13C detection to study intrinsically disordered proteins. J. Magn. Reson. 2014, 241, 115-125.
14. Lopez, J.; Schneider, R.; Cantrelle, F.-X.; Huvent, I.; Lippens, G., Studying Intrinsically Disordered Proteins under True In Vivo Conditions by Combined Cross-Polarization and Carbonyl-Detection NMR Spectroscopy. Angew. Chem., Int. Ed. 2016, 128, 7544-7548.

15. Sukumaran, S.; Malik, S. A.; R., S. S.; Chandra, K.; Atreya, H. S., Rapid NMR assignments of intrinsically disordered proteins using two-dimensional 13C-detection based experiments. Chem. Commun. 2019, 55, 7820-7823.

16. Wang, A. C.; Grzesiek, S.; Tschudin, R.; Lodi, P. J.; Bax, A., Sequential backbone assignment of isotopically enriched proteins in D2O by deuterium-decoupled HA(CA)N and HA(CACO)N. J. Biomol. NMR 1995, 5, 376-382.

17. Kanelis, V.; Donaldson, L.; Muhandiram, D. R.; Rotin, D.; Forman-Kay, J. D.; Kay, L. E., Sequential assignment of proline-rich regions in proteins: Application to modular binding domain complexes. J. Biomol. NMR 2000, 16, 253-259.

18. Mäntylahti, S.; Aitio, O.; Hellman, M.; Permi, P., HA-detected experiments for the backbone assignment of intrinsically disordered proteins. J. Biomol. NMR 2010, 47, 171-181.

19. Mäntylahti, S.; Hellman, M.; Permi, P., Extension of the HA-detection based approach: (HCA)CON(CA)H and (HCA)NCO(CA)H experiments for the main-chain assignment of intrinsically disordered proteins. J. Biomol. NMR 2011, 49, 99-109.

20. Dudás, E. F.; Pálfy, G.; Menyhárd, D. K.; Sebák, F.; Ecsédi, P.; Nyitray, L.; Bodor, A., Tumor-Suppressor p53TAD(1-60) Forms a Fuzzy Complex with Metastasis-Associated S100A4: Structural Insights and Dynamics by an NMR/MD Approach. ChemBioChem 2020.

21. Brüschweiler, R.; Griesinger, C.; Sørensen, O. W. W.; Ernst, R. R. R., Combined use of hard and soft pulses for ω1decoupling in two-dimensional NMR spectroscopy. J. Magn. Reson. 1988, 78, 178-185.

22. Zangger, K., Pure shift NMR. Prog. Nucl. Magn. Reson. Spectrosc. 2015, 86-87, 1-20.

23. Castañar, L.; Parella, T., Broadband 1H homodecoupled NMR experiments: recent developments, methods and applications. Magn. Reson. Chem. 2015, 53, 399-426.

24. Anderson, W. A.; Freeman, R., Influence of a Second Radiofrequency Field on High-Resolution Nuclear Magnetic Resonance Spectra. J. Chem. Phys. 1962, 37, 85-103.

25. Hammarström, A.; Otting, G., Improved Spectral Resolution in 1H NMR Spectroscopy by Homonuclear Semiselective Shaped Pulse Decoupling during Acquisition. J. Am. Chem. Soc. 1994, 116, 8847-8848.

26. Kupče, Ē.; Freeman, R.; Wider, G.; Wüthrich, K., Suppression of Cycling Sidebands Using Bi-level Adiabatic Decoupling. J. Magn. Reson. A 1996, 122, 81-84.

27. Aue, W. P.; Karhan, J.; Ernst, R. R., Homonuclear broad band decoupling and two-dimensional J-resolved NMR spectroscopy. J. Chem. Phys. 1976, 64, 4226-4227.

28. Pell, A. J.; Keeler, J., Two-dimensional J-spectra with absorption-mode lineshapes. J. Magn. Reson. 2007, 189, 293-299.

29. Luy, B., Adiabatic z-filtered J-spectroscopy for absorptive homonuclear decoupled spectra. J. Magn. Reson. 2009, 201, 18-24.

30. Zangger, K.; Sterk, H., Homonuclear Broadband-Decoupled NMR Spectra. J. Magn. Reson. 1997, 124, 486-489.

31. Sakhaii, P.; Haase, B.; Bermel, W., Experimental access to HSQC spectra decoupled in all frequency dimensions. J. Magn. Reson. 2009, 199, 192-198.

32. Aguilar, J. A.; Nilsson, M.; Morris, G. A., Simple Proton Spectra from Complex Spin Systems: Pure Shift NMR Spectroscopy Using BIRD. Angew. Chem., Int. Ed. 2011, 50, 9716-9717.

33. Görling, B.; Bräse, S.; Luy, B., HR-HSBC: Measuring heteronuclear one-bond couplings with enhanced resolution. Magn. Reson. Chem. 2012, 50, 58-62.

34. Lupulescu, A.; Olsen, G. L.; Frydman, L., Toward single-shot pure-shift solution 1H NMR by trains of BIRD-based homonuclear decoupling. J. Magn. Reson. 2012, 218, 141-146.

35. Castañar, L.; Nolis, P.; Virgili, A.; Parella, T., Full Sensitivity and Enhanced Resolution in Homodecoupled Band-Selective NMR Experiments. Chem. Eur. J. 2013, 19, 17283-17286.

36. Meyer, N. H.; Zangger, K., Simplifying proton NMR spectra by instant homonuclear broadband decoupling. Angew. Chem., Int. Ed. 2013, 52, 7143-7146.

37. Reinsperger, T.; Luy, B., Homonuclear BIRD-decoupled spectra for measuring one-bond couplings with highest resolution: CLIP/CLAP-RESET and constant-time-CLIP/CLAP-RESET. J. Magn. Reson. 2014, 239, 110-120.

38. Ying, J.; Roche, J.; Bax, A., Homonuclear decoupling for enhancing resolution and sensitivity in NOE and RDC measurements of peptides and proteins. J. Magn. Reson. 2014, 241, 97-102.

39. Meyer, N. H.; Zangger, K., Enhancing the resolution of multi-dimensional heteronuclear NMR spectra of intrinsically disordered proteins by homonuclear broadband decoupling. Chem. Commun. 2014, 50, 1488-1490.

40. Kiraly, P.; Adams, R. W.; Paudel, L.; Foroozandeh, M.; Aguilar, J. A.; Timári, I.; Cliff, M. J.; Nilsson, M.; Sándor, P.; Batta, G.; Waltho, J. P.; Kövér, K. E.; Morris, G. A., Real-time pure shift 15N HSQC of proteins: a real improvement in resolution and sensitivity. J. Biomol. NMR 2015, 62, 43-52.

41. Foroozandeh, M.; Adams, R. W.; Kiraly, P.; Nilsson, M.; Morris, G. A., Measuring couplings in crowded NMR spectra: pure shift NMR with multiplet analysis. Chem. Commun. 2015, 51, 15410-15413.

42. Sinnaeve, D.; Foroozandeh, M.; Nilsson, M.; Morris, G. A., A General Method for Extracting Individual Coupling Constants from Crowded 1H NMR Spectra. Angew. Chem., Int. Ed. 2016, 55, 1090-1093.

43. Reller, M.; Wesp, S.; Koos, M. R. M.; Reggelin, M.; Luy, B., Biphasic Liquid Crystal and the Simultaneous Measurement of Isotropic and Anisotropic Parameters by Spatially Resolved NMR Spectroscopy. Chem. Eur. J. 2017, 23, 13351-13359.

44. Görling, B.; Bermel, W.; Bräse, S.; Luy, B., Homonuclear decoupling by projection reconstruction. Magn. Reson. Chem. 2018, 56, 1006-1020.

45. Haller, J. D.; Bodor, A.; Luy, B., Real-time pure shift measurements for uniformly isotope-labeled molecules using X-selective BIRD homonuclear decoupling. J. Magn. Reson. 2019, 302, 64-71.

46. Kobzar, K.; Ehni, S.; Skinner, T. E.; Glaser, S. J.; Luy, B., Exploring the limits of broadband 90° and 180° universal rotation pulses. J. Magn. Reson. 2012, 225, 142-160.

47. Skinner, T. E.; Gershenzon, N. I.; Nimbalkar, M.; Bermel, W.; Luy, B.; Glaser, S. J., New strategies for designing robust universal rotation pulses: Application to broadband refocusing at low power. J. Magn. Reson. 2012, 216, 78-87.

48. Smith, M. A.; Hu, H.; Shaka, A. J., Improved Broadband Inversion Performance for NMR in Liquids. J. Magn. Reson. 2001, 151, 269-283.

49. Kobzar, K.; Skinner, T. E.; Khaneja, N.; Glaser, S. J.; Luy, B., Exploring the limits of broadband excitation and inversion pulses. J. Magn. Reson. 2004, 170, 236-243.

50. Kobzar, K.; Skinner, T. E.; Khaneja, N.; Glaser, S. J.; Luy, B., Exploring the limits of broadband excitation and inversion: II. Rf-power optimized pulses. J. Magn. Reson. 2008, 194, 58-66.

51. Ehni, S.; Luy, B., BEBEtr and BUBI: J-compensated concurrent shaped pulses for 1H-13C experiments. J. Magn. Reson. 2013, 232, 7-17.

52. Geen, H.; Freeman, R., Band-selective radiofrequency pulses. J. Magn. Reson. 1991, 93, 93-141.

53. Vuister, G. W.; Bax, A., Resolution enhancement and spectral editing of uniformly 13C-enriched proteins by

homonuclear broadband 13C decoupling. J. Magn. Reson. 1992, 98, 428-435.

54. Maltsev, A. S.; Ying, J.; Bax, A., Deuterium isotope shifts for backbone 1H, 15N and 13C nuclei in intrinsically disordered protein α-synuclein. J. Biomol. NMR 2012, 54, 181-191.

55. Alik, A.; Bouguechtouli, C.; Julien, M.; Bermel, W.; Ghouil, R.; Zinn-Justin, S.; Theillet, F.-X., Sensitivity-Enhanced 13C-NMR Spectroscopy for Monitoring Multisite Phosphorylation at Physiological Temperature and pH. Angew. Chem., Int. Ed. 2020, 2.

56. Nath, J.; Smith, T.; Hollis, A.; Ebbs, S.; Canbilen, S. W.; Tennant, D. A.; Ready, A. R.; Ludwig, C., 13C glucose labelling studies using 2D NMR are a useful tool for determining ex vivo whole organ metabolism during hypothermic machine perfusion of kidneys. Transplant. Res. 2016, 5, 7.

57. Schätzlein, M. P.; Becker, J.; Schulze-Sünninghausen, D.; Pineda-Lucena, A.; Herance, J. R.; Luy, B., Rapid two-dimensional ALSOFAST-HSQC experiment for metabolomics and fluxomics studies: application to a 13C-enriched cancer cell model treated with gold nanoparticles. Anal. Bioanal. Chem. 2018, 410 (11), 2793-2804.

58. Saborano, R.; Eraslan, Z.; Roberts, J.; Khanim, F. L.; Lalor, P. F.; Reed, M. A. C.; Günther, U. L., A framework for tracer-based metabolism in mammalian cells by NMR. Sci. Rep. 2019, 9 (1), 2520.

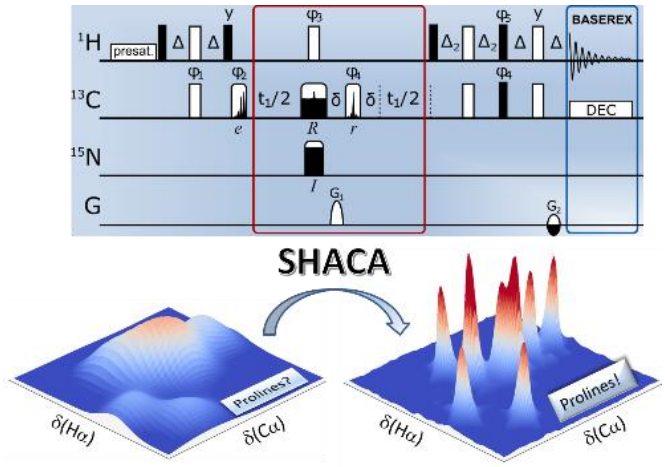

The power of pure shift HαCα correlations: a new way to characterize biomolecules under physiological conditions

Andrea Bodor, Jens D. Haller, Chafiaa Bouguechtouli, Francois-Xavier Theillet, László Nyitray, Burkhard Luy**